Decisions on the basis of continuous accumulation of memory and sensory evidence.

Aaron M. Bornstein[1,*], Mariam Aly[1], Samuel F. Feng[3],
Nicholas B. Turk-Browne[1,2], Kenneth A. Norman[1,2], Jonathan D. Cohen[1,2]

1. Neuroscience Institute, Princeton University, Princeton, NJ, USA

2. Department of Psychology, Princeton University, Princeton, NJ, USA

3. Department of Applied Mathematics and Sciences, Khalifa University, Abu Dhabi, UAE

* To whom correspondence should be addressed: aaronmb@princeton.edu.

Abstract

How does what we expect to see influence what we perceive? Previous research has shown that perceptual decisions can be made on the basis of prior expectations combined with sensory input. To date, these expectations have been treated as static, received quantities. Here, we tested the hypothesis that expectations can themselves be inferred using dynamic evidence accumulation, in a process continuous with that of sensory inference. In two experiments using a novel cue-guided perceptual decision task that separately varied the information available to expectations and perception, we tested the degree to which decisions reflected accumulation of both kinds of information. In Experiment 1, we found that participants' response times and choices matched the quantitative and qualitative predictions of a two-stage evidence accumulation model. In Experiment 2, participants performed the same task while being scanned in fMRI. Using neural pattern analysis, we measured the expectations that participants formed in advance of sensory information, and found that these trial-specific expectations reliably predicted the speed of responding to sensory input. These results demonstrate that perceptual decisions rely on a continuous process of evidence accumulation, that begins even before perceptual information is available.

How do we combine memory and perception to make decisions? Laboratory studies of decision-making tend to focus on choices made on the basis of a single kind of information alone, such as anticipated utility [1], sensory input [2], or mnemonic evidence [3, 4]. But in the real world, our decisions depend on integrating all available information.

For instance, if, when traveling by train, I miss my stop, how do I figure out which station will allow me to transfer towards home? I could rely solely on sight – as the train stops at each station, quickly scan the platform for helpful signs or markings. I could rely solely on my memories – which station is next? Will it have the transfer I need? Both kinds of information can be unreliable: station platforms may look very similar, with distant or

unhelpful signage, or my memories could be few, sparse, and unclear. More likely, I will combine both kinds of information: query my memories about which stations might have transfers, and combine those with what I can see from a quick look out the door at each stop. By combining the expectations, derived from memory, with visual information, I can improve my ability to figure out where I am, and thus where I need to go.

An open question in the study of perceptual decisions is how expectations should, and do, influence the inference process. Empirical studies and theoretical work have focused on incorporating expectations within the canonical evidence accumulation framework [2, 3]. To date, the field has diverged on the question of whether expectations result in a change to the starting point or rate of evience accumulation [5–8], or a more dynamic influence that increases as a decision takes longer to resolve [9].

However, all of these approaches assume that the content of expectations is fixed before the decision starts, whether by learning or by instruction. In the train analogy, the map is known with certainty, though the reliability of the visual cues vary from station to station (trial to trial).

Here, we propose that expectations can also be set by a dynamic evidence accumulation process. This process is set in motion by a predictive cue about an upcoming stimulus, and begins before the stimulus is seen. This dynamic inference process, operating on expectations, informs the dynamic inference process operating on sensory evidence.

In doing so, we recast this debate by considering the fact that perceptual (and memory) decisions are a special case of a broader class of problems, known as *state inference* [10]. Treating the problem as one of state inference, we can approach other kinds of information – here, memories – as potentially informative evidence that can be integrated alongside sensory input, to guide action selection.

We and others have previously suggested that decisions can be made on the basis of memories sampled in a manner captured by the sorts of evidence accumulation models used to investigate perceptual decisions [3, 11–14]. Building on this work, we test the hypothesis that perceptual decisions can arise from a continuous accumulation process that incorporates multiple types of evidence as they become available, and to the extent that they are useful.

Our hypothesis yields two key predictions. First, when new information becomes available, evidence accumulation should undergo an inflection, in the direction of the new evidence, and to the degree that the new information is useful. Second, evidence accumulated before the onset of new information should affect decisions made on the basis of that new information. The predictions of the hypothesis are formalized using a new, two-stage evidence accumulation model [15], which diverges from the above proposals in that expectations are dynamic, constructed at the time of decision, and thus their effect can vary between trials, depending on how reliable and consistent are the experiences from which they are constructed, as well as to what degree those experiences match sensory information. The model, by integrating information across modalities and making decisions based on their superposition, also diverges from "race" models [16] that cast action selection as a competition between parallel, non-interacting accumulators.

To test our predictions, we developed a memory-guided perceptual inference task. In the

task, two distinct kinds of decision-relevant information – memory and perceptual input – are each made available at separate times. A fractal cue probabilistically signals the likely identity, and reliability, of a noisy percept, which follows a few seconds later. Critically, in this task responses may be selected on the basis of one, or both types of information.

Experiment 1 tests the first prediction, investigating whether behavior reflects the continuous, integrative, accumulation of both types of information. In Experiment 2, we used fMRI and multivariate pattern analysis (MVPA) to measure, on a trial-by-trial basis, neural evidence for accumulation from memory, in advance of the availability of perceptual information. This measure allows us to test the second prediction, by examining whether accumulated memory evidence influences decisions made after perceptual information is available.

Taken together, these experiments open a new line of investigation in the study of perceptual decisions, by demonstrating a potentially critical role for dynamic inference from memory, as well as sensory, information. Further, they motivate further investigation into evidence accumulation, throughout the brain, that integrates other forms of internal and external signals in a cooperative, rather than competitive, fashion.

Results

Participants performed a cue-guided perceptual inference task (Figure 1a,b), in which fractal cues could be used to anticipate the content of a noisy perceptual stimulus. Each of four fractal cues signaled, with probability between 50% and 80%, which photographs would follow after a short inter-stimulus interval (ISI). The photographs were split into two categories: faces and scenes. In the *Learning* phase (Figure 1a), participants learned, by experience, the likelihood that each fractal would be followed by one of two same-category photographs.

In the *Test* phase, (Figure 1b), the fractals were now followed by a noisy, "flickering" stream, consisting of two rapidly alternating same-category photographs. On these trials, the cues predicted the identity of the *target* photograph – the one that would be shown most often in the flickering stream. We varied the reliability of the perceptual information such that the target photograph would be shown on a higher or lower proportion of frames. The reliability was set by category – on some experiment runs, faces might be easier to discriminate than scenes, or vice-versa. In both phases, participants were instructed only to press the key associated with each photograph (key-photograph pairings were fixed, and learned in a separate training phase). Importantly, however, participants could respond before stimulus onset; the cue allowed participants to anticipate the upcoming photograph, and decide whether or not to use this information to respond before the stimulus appeared.

Most participants performed the task twice, in *blocks* with different photographs, fractals, cue-photograph probabilities, and category-coherence mappings.

Due to time limitations or technical problems, some participants only completed one block (see *Methods* for details). In Experiment 1, 30 participants together completed 56 total blocks. In Experiment 2, a separate set of 31 participants performed the same task in an fMRI scanner, completing 52 blocks in total. Because participants completed different, randomly-assigned, subsets of the task conditions (the four cue and coherence levels), statistics on the

correlations between task conditions and dependent measures are computed by bootstrap across participants.

Experiment 1

Response times and accuracy

Responses reflect cue predictions and perceptual evidence. Participants responded with high accuracy, and with response times reflecting the quality of information available from both the fractal cue and the perceptual stream. On average, across all participant-blocks, correct responses (defined only on trials for which there was a "correct" response defined before stimulus onset – i.e. for cue levels 0.6, 0.7, 0.8) were high (75.20% (SEM 0.085%), and reliably greater than chance for all blocks individually (all $p \leq 0.0465$ by binomial test). Accuracy increased with both cue predictiveness ($R = 0.1947$, $P = 0.009$ by bootstrap across participants; Figure 2a) and coherence ($t(27) = -4.4297$, $P = 0.0001$; defined only for the 28 subjects who performed at least one block in which there was a correct response in both coherence conditions).

Participants used the fractal cue to decide whether or not to respond "early", before the onset of the perceptual stimulus ($R = 0.2224$, bootstrap $P < 0.0001$; Figure 2b). This relationship was driven by trials on which the cue signaled that the perceptual stimulus would be of low coherence (for low coherence trials, $R = 0.3658$, bootstrap $P < 0.0001$; high-coherence trials $R = 0.0868$, bootstrap $P = 0.1610$; difference between paired bootstrap iterations reliable with Cohen's $d = 3.9071$).

Reflecting the two-stage nature of the integration task, response times were distinctly bimodal, with separate peaks following the onsets of the fractal cue and the flickering stimulus (Figure 3a; all groups multimodal by Hartigan's Dip Test [17]: all HDS$\geq$ 0.0281, all $P <$ 0.0001).

Early responses were speeded by cue predictions, but not by (anticipated) perceptual coherence. Across all conditions, these early RTs showed a trend towards being faster as the fractal was more predictive ($R = -0.0351$, $P = 0.086$ by bootstrap across participants). Consistent with the normative prediction that uninformative cues discourage deliberation [18], this relationship was reliable when including only informative cues (60% and higher; $R = -0.0501$, bootstrap $P = 0.008$). Though early response speeds did not differ between coherence levels, (mean RTs – cue-locked, log-transformed, Z-scored within subject: 0.65: $-0.0072 SEM 0.0617$; 0.85: 0.0307 SEM 0.0597; mean difference -0.0383 SEM 0.1061, $t(22) = -0.3607$, $P = 0.7217$; defined only for the 23 subjects who made early responses at both coherence levels), the relationship between cue and early RT was present at both coherence levels (0.65: $R = -0.1192$, bootstrap $P = 0.023$; 0.85: $R = -0.1536$, bootstrap $P < 0.0001$),

Post-stimulus responses were speeded by cue predictiveness ($R = -0.017$, bootstrap $P = 0.044$; Figure 2c), and also by coherence (mean RTs – stimulus-locked, log-transformed, Z-scored within subject: 0.65: 0.1581 SEM 0.0612 0.85: -0.1283 SEM 0.0387 mean difference 0.2864 SEM 0.0911; $t(29) = 3.145$, $P = 0.0038$). These relationships were interactive:

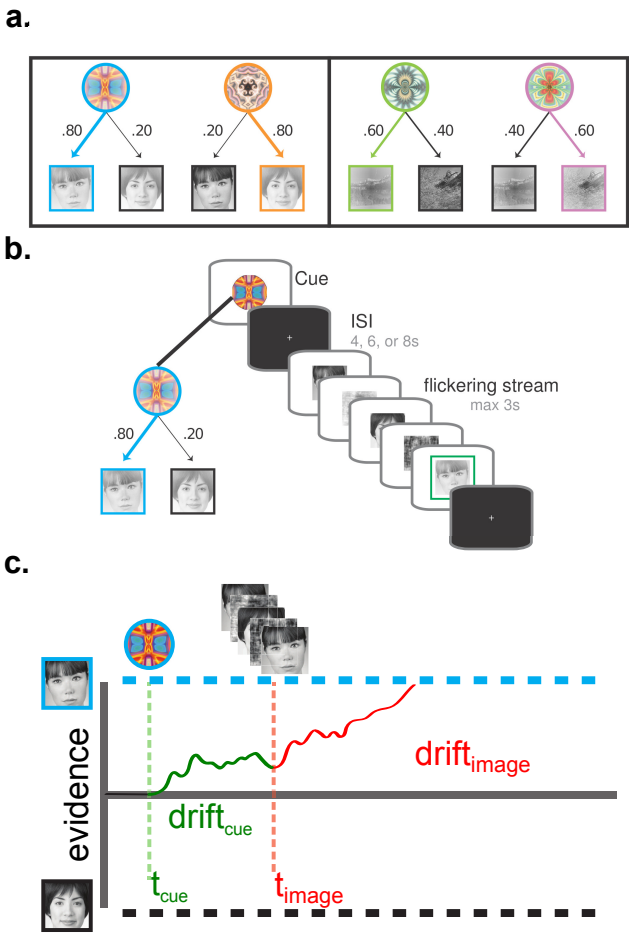

Figure 1: **Cue-guided perceptual inference task**. **(a)** In the *Cue-stimulus learning* phase, participants performed 100 trials to learn which face or scene stimulus was predicted by each of four fractal cues. Each cue was shown 25 times, and at each presentation it was followed by a picture of either a face or a scene. Cues were linked to one category only, and to each picture within that category according to complementary proportions (50%/50%, 60%/40%, 70%/30%, 80%/20%). **(b)** On trials in the *Perceptual decision* phase, participants were again shown a fractal cue, but in this case the cue was followed by a "flickering" series of stimulus pictures alternated rapidly (60Hz). Each frame of the series contained either one of the two pictures from the cued category, or a phase-scrambled version of the previously-shown picture. One picture, the *target*, was shown in the stream more often than the other. The fraction of frames that contained the target picture was either high or low, at a ratio calibrated to elicit higher or lower accuracy. Participants were asked to respond by pressing the key associated with the picture most often shown. Critically, they were allowed to respond before the picture appeared on screen. These "early" responses allowed us to observe their decision to rely on memory evidence alone. **(c)** Two-stage continuous accumulation model. The *Multi-Stage Drift-Diffusion Model* (MSDDM) describes an evidence accumulation process with time-varying drift rate [15]. The first drift rate corresponds to the period following onset of the fractal cue and preceding the onset of the flickering image stream, while the second corresponds to the period after the onset of the flickering image stream. Critically, the end point of the first stage sets the starting point of the second.

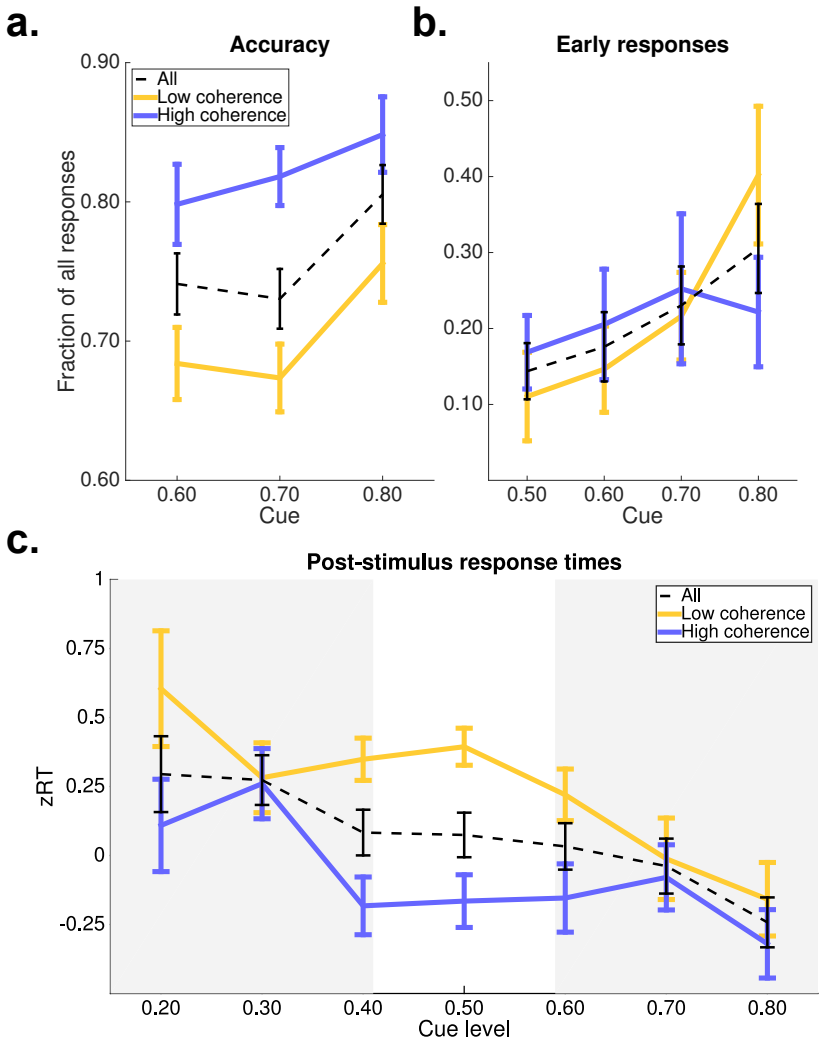

Figure 2: **Early responses and accuracy scale with cue predictiveness and perceptual coherence**. **(a)** Participants were more likely to respond early when the fractal cue made a more reliable prediction about the identity of the upcoming stimulus ($R = 0.2224$, bootstrap $P < 0.0001$). This relationship was stronger when participants knew that the upcoming stimulus would be of low coherence (0.65: $R = 0.3658$, bootstrap $P < 0.0001$; 0.85: $R = 0.0868$, bootstrap $P = 0.161$; Cohen's $d = 2.3841$). **(b)** Across all trials, accuracy increased with cue reliability ($R = 0.1947$, bootstrap $P = 0.005$), and with the coherence of the flickering stream ($t(27) = -4.4297$, $P = 0.0001$). **(c)** When perceptual evidence was of high coherence, participant responses after the onset of the flickering stream were faster than on low-coherence trials ($t(29) = 3.145$, $P = 0.0038$). Across all such responses, response time decreased with the cued probability of the target photograph ($R = -0.017$, bootstrap $P = 0.044$). This relationship was stronger for low-coherence trials (0.65: $R = -0.147$, bootstrap $P < 0.0001$; 0.85: $R = -0.065$, bootstrap $P = 0.033$; Cohen's $d = 1.7385$), and for trials where the target photograph matched the one predicted by the fractal cue – cue $0.6 - 0.8$ (right shaded region): $R = -0.063$, bootstrap $P < 0.001$; cue $0.2 - 0.4$ (left shaded region): $R = 0.0419$, bootstrap $P = 0.141$; Cohen's $d = 1.7385$).

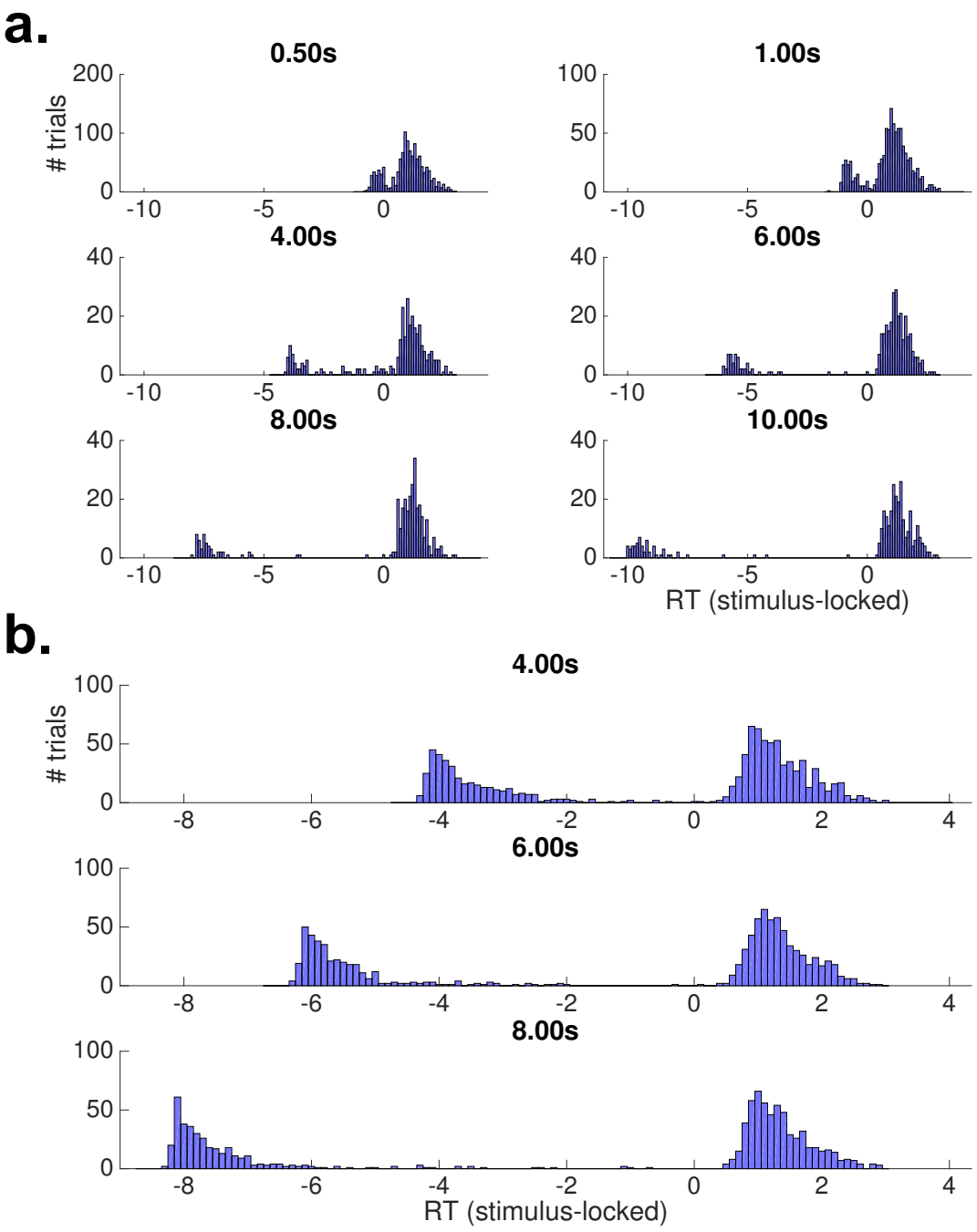

Figure 3: **Histogram of (stimulus-locked) response times on test-phase trials**. RT counts are aggregated across participants, and plotted separately for each ISI condition, binned in increments of 100ms Separate peaks follow the onset of the fractal cue and the onset of the flickering stream, reflecting the fact that participants made responses on the basis of both types of information. **(a)** Experiment 1, ISIs of 500ms, 1s, 4s, 6s, 8s, 10s. **(b)** Experiment 2, ISIs of 4s, 6s, 8s.

participants were more speeded by cue predictiveness when coherence was lower (0.65: $R = -0.147$, bootstrap $P < 0.0001$; 0.85: $R = -0.065$, bootstrap $P = 0.033$; Cohen's $d = 1.675$), and only when the target photograph matched the cue's prediction: (incongruent: $R = 0.0419$, bootstrap $P = 0.141$; congruent: $R = -0.063$, bootstrap $P < 0.001$; Cohen's $d = 1.7385$).

Taken together, these results confirm that participants' responses reflected a dynamic integration of their memories about which photograph followed each cue with the experienced (and anticipated) sensory information.

Model comparison

We used model comparison to formally test the hypothesis that responses resulted from a two-stage evidence accumulation process – the first on the basis of the cue, and preceding the flickering stimulus, the second following the onset of the flickering series. Our primary model of interest implemented a continuous, two-stage evidence accumulation process (hereafter: MSDDM; [15]; Figure 1c), with distinct drift rates for evidence integrated within each stage.

Our aim was to determine whether participants' responses reflected key qualitative features that distinguish the MSDDM: namely, that the drift rate changed at the time of flickering stream onset, and that accumulation in the second stage proceeded from the evidence accumulated during the first stage. Therefore, our comparisons were against sampling models that selectively disabled each of those features. The first comparison model was a single DDM, which had continuous accumulation until the time of response, but no change in drift rate across the entire trial. We refer to this model as *1DDM*. The second comparison model was two unconnected DDMs, mirroring the change in drift rate found in MSDDM, but with the second-stage starting point set independently of the behavior of the first model. We refer to this model as *2DDM*. Each model was fit to responses aggregated, across subjects, by cue and coherence condition.

Against the second-best model, the 2DDM model, MSDDM was superior by a BIC of 30 (constituting "Strong" evidence in favor of the model, according to [19]). This was the case across all conditions, and for nearly every condition individually (Figure 4a). (Parameter fits for each model can be found in Supplemental Tables 1–3.)

Experiment 2

Experiment 1 showed that aggregate behavior in this task reflects a dynamic integration of memory and sensory evidence, yielding patterns of choices and response times that are best captured by the MSDDM. In Experiment 2, we used fMRI to test whether accumulated memory evidence could be used to predict responses on an individual trial basis. For this experiment, 31 additional participants completed the task from Experiment 1, while being scanned for fMRI.

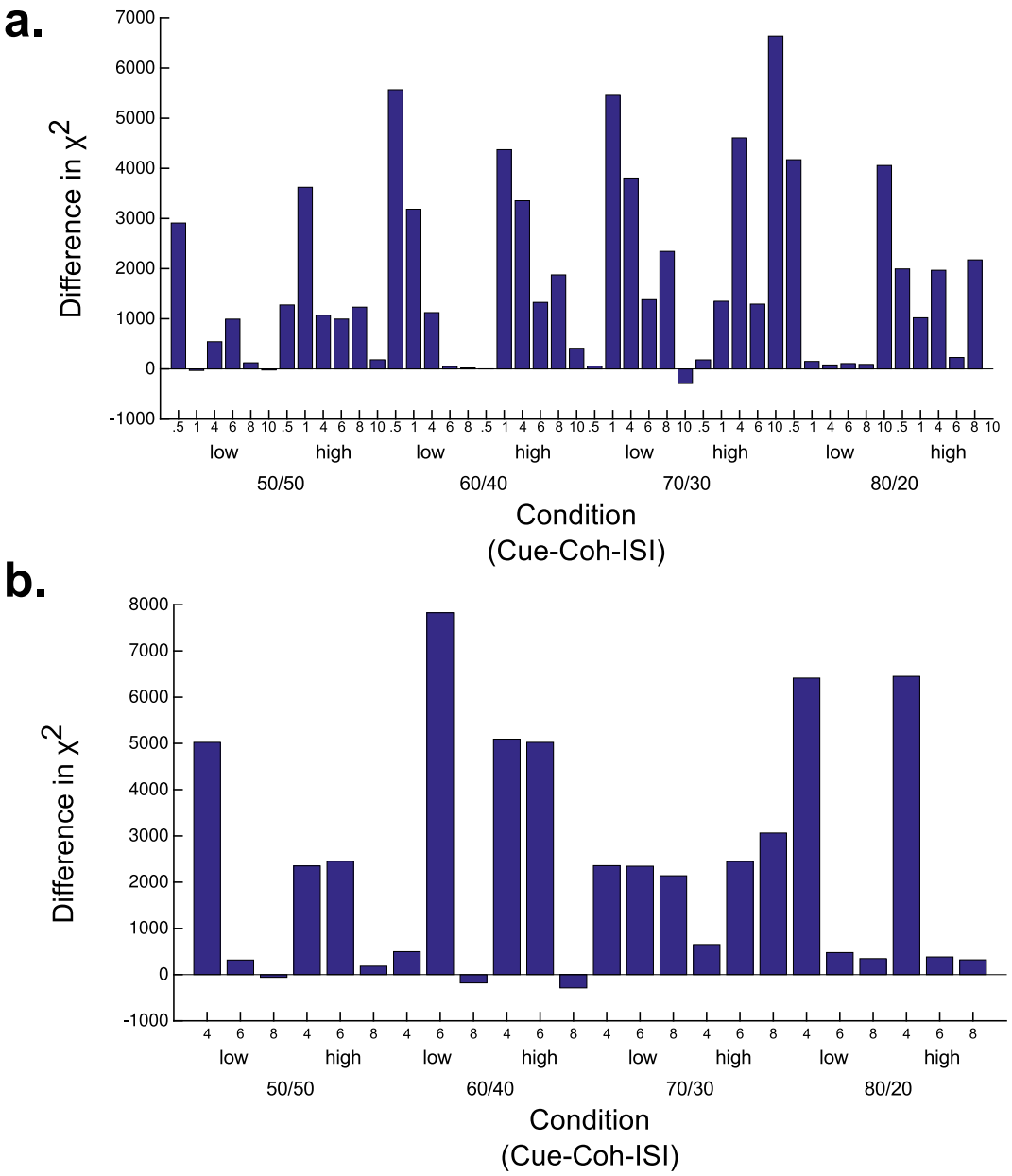

Figure 4: **Model comparison**. Models were compared for their fit to each bin of trials with the same combination of cue predictiveness, perceptual coherence, and ISI. Shown here is the χ^2 difference in favor of the MSDDM model (higher bar = greater evidence in favor MSDDM), for each trial bin. MSDDM was favored over 2DDM for nearly every condition individually, and across all conditions as a whole. **(a)** Experiment 1 **(b)** Experiment 2

Behavior

Response times and accuracy.

Accuracy was again high overall – 70.24% correct responses (SEM 1.18%); significant or trending for 49/52 blocks individually (all $p \leq 0.0728$).

Accuracy again increased with cue predictiveness ($R = 0.2474$, bootstrap $P = 0.005$) and coherence ($t(26) = -4.3017$, $P = 0.0002$). Response times were bimodal (all HDS≥ 0.1017, all $P < 0.0001$; Figure 3b). Higher cue predictiveness lead both to a greater tendency to respond early ($R = 0.1494$, bootstrap $P = 0.012$), though this time the effect was driven by high-coherence trials (0.65: $R = -0.1022$, bootstrap $P = 0.111$; 0.85: $R = 0.4187$, bootstrap $P < 0.0001$; Cohens $d = 4.2134$), perhaps reflecting that early responding was at ceiling when participants anticipated low coherence stimuli. Cue predictiveness also caused early responses to be faster $R = -0.0768$, bootstrap $P < 0.0001$); an effect that was equally strong across coherence levels (0.65: $R = -0.2309$, bootstrap $P < 0.0001$; 0.85: $R = -0.2285$, bootstrap $P < 0.0001$; Cohen's $d = -0.1609$).

Responses after the onset of the flickering stimulus were again speeded by coherence (0.65: 0.2268 SEM 0.0421; 0.85: -0.0981 SEM 0.0782; mean difference 0.3248 SEM 0.0977; $t(30) = 3.3255$, $P = 0.0023$), and by cue predictiveness, in both coherence conditions (0.65: $R = -0.0921$, bootstrap $P = 0.021$; 0.85: $R = -0.0599$, bootstrap $P = 0.013$), though moreso when coherence was lower (Cohen's $d = 0.7604$), and when the target photograph matched the cue's prediction: (incongruent: $R = 0.0249$, bootstrap $P = 0.303$; congruent: $R = -0.0165$, bootstrap $P = 0.191$; Cohen's $d = 0.9447$).

Finally, model comparison again favored the MSDDM over the alternative candidate models (all BIC > 21; Figure 4b; fitted parameters in Supplemental Tables 4–6).

Neuroimaging pattern analysis

We used neural pattern similarity to measure the influence of accumulated memory evidence on responses. For each participant, we defined, on the basis of a post-task face/scene localizer, regions in the ventral visual stream that were more active for face versus scene processing (FFA; [20]) and more activity for scene versus face processing (PPA; [21]) (Figure 5a). We next used the data from Phase 2 response-learning trials to compute *target patterns*: activity corresponding to each photograph, in the appropriate category-preferring region (faces in FFA, scenes in PPA). Critically, because Phase 2 preceded the introduction of the fractal cues, these patterns were decoupled from the fractals.

We next computed, for each test-phase trial, the *trial pattern* – the average activity in these regions over the period following the onset of the fractal cue, up to either the participant's response, or one TR before the onset of the flickering stream, whichever came first. Hereafter, we define the trial-by-trial *reinstatement index* as the correlation between these trial patterns and the target pattern corresponding to the photograph predicted by the fractal cue. (Note that on 50/50 trials, this value is not defined.)

Pre-stimulus reinstatement scales with task conditions.

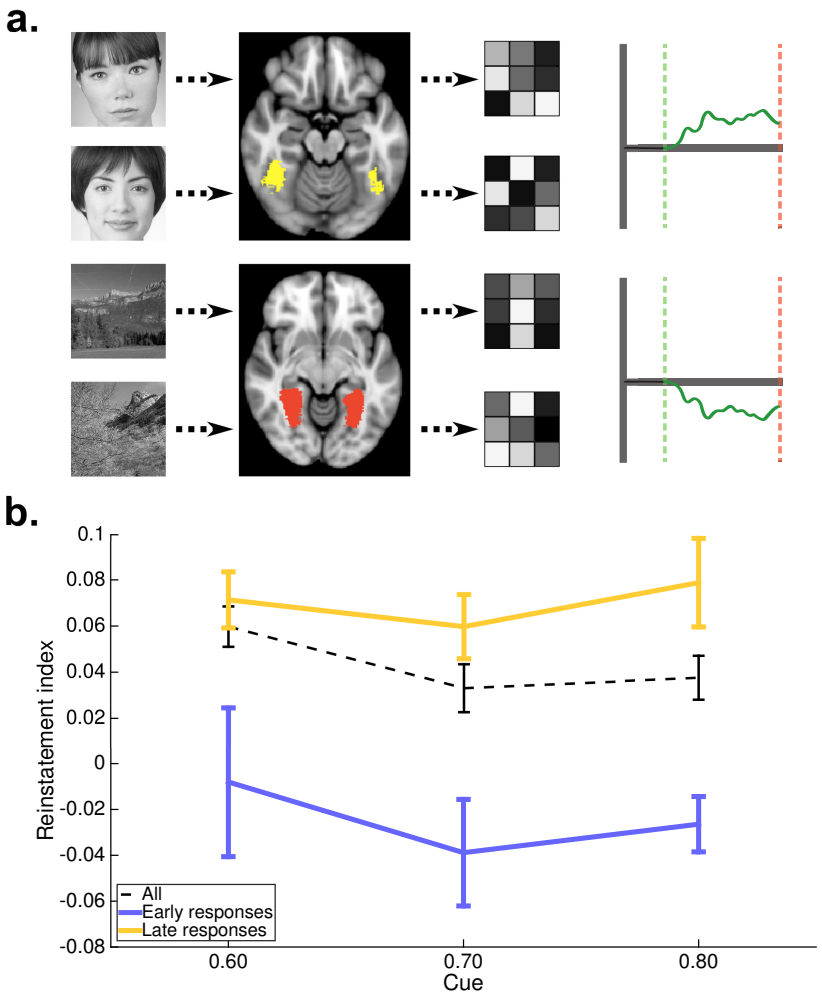

Figure 5: **Reinstatement pattern analysis**. **(a)** We defined, for each participant, the Fusiform Face Area (FFA) and Parahippocampal Place Area (PPA), using a localizer task that followed the main experiment. The resulting mask defined the region across which we calculated picture-specific template. Next, for each trial on which participants responded after the onset of the flickering stream, we computed the average activity in the corresponding ROI over the period following the onset of the fractal cue, but preceding the onset of that flickering stream. The *reinstatement index* is the correlation between this trial-specific pattern and the picture-specific pattern corresponding to the picture predicted by the fractal cue. **(b)** Reinstatement index scales with cue predictiveness. As the cue triggered more reliable memories, reinstatement index was lower, ($R = -0.0341$, bootstrap $P = 0.039$), consistent with an evidence accumulation process that reached bound more quickly, under the temporal resolution of the BOLD response However, on trials where participants responded after the onset of the perceptual stimulus, accumulation did not, by definition, terminate. Thus, on these trials, there was no relationship between cue predictiveness and reinstatement index no such correlation was observed for late responses ($R = 0.0203$, bootstrap $P = 0.225$).

As in a previous study of memory sampling [11], we expected that anticipatory stimulus reinstatement would scale negatively with cue probability. The reason for this is that in evidence accumulation models, samples are accumulated until a threshold is reached in favor of a given response. At that point, no more sampling – and thus no more activity linked to memory reinstatement – should follow. Because memory sampling likely occurs at a timescale below the resolution of the BOLD response [22], more predictive cues should lead to less consistent trial patterns, and thus a lower correlation with the template pattern. Consistent with the prediction, reinstatement index decreased as cue probability increased ($R = -0.0341$, bootstrap $P = 0.039$; Figure 5b).

Following the same logic, this relationship should only hold for early responses – by definition trials on which accumulation terminates in the time period we are measuring – but not on trials where the participant responded following stimulus onset – those on which accumulation continues until stimulus onset. Indeed, while the correlation between cue probability and reinstatement index was reliably negative for early response trials ($R = -0.0718$, bootstrap $P = 0.004$), no such correlation was observed for late responses ($R = 0.0203$, bootstrap $P = 0.225$; difference between paired bootstrap iterations Cohen's $d = 1.7417$).

Pre-stimulus reinstatement predicts 2nd stage response times. The fact that reinstatement index is related to cue probability is consistent with evidence accumulation models, but does not differentiate between MSDDM versus 1DDM or 2DDM. The key test of the MSDDM is whether responses to the flickering stream are influenced by evidence accumulation in anticipation of sensory input. Therefore, we tested reinstatement index could predict response times after the onset of the flickering stream, on each specific trial.

Supporting the hypothesis, reinstatement index was indeed associated with faster post-stimulus response times ($R = -0.0700$, bootstrap $P = 0.001$), a relationship that held after controlling for other factors (cue level, coherence, ISI, on-screen evidence) that also modulate response times ($R = -0.0337$, bootstrap $P = 0.039$; Figure 6a). Further, consistent with the predication that accumulated memory evidence sets the starting point for perceptual accumulation, reinstatement index only speeded response times on trials where the cue's prediction was valid: (cue-incongruent: $R = 0.0096$, bootstrap $P = 0.404$; cue-congruent: $R = -0.0527$, bootstrap $P = 0.029$; Cohen's $d = -1.2037$; Figure 6b), driven by the divergence in its effect on cue-congruent and cue-incongruent trials in the low-coherence condition: (low coherence, cue-incongruent: $R = 0.127$, bootstrap $P = 0.087$; low coherence, cue-congruent: $R = -0.0384$, bootstrap $P = 0.161$; Cohen's $d = -1.586$; Figure 6c), and matching the sort of reliability-weighted integration predicted by the two-stage evidence accumulation model.

Together, these results support a role in perceptual decisions for the dynamic accumulation of memory evidence, and for a continous inference process linking memory, perception, and action.

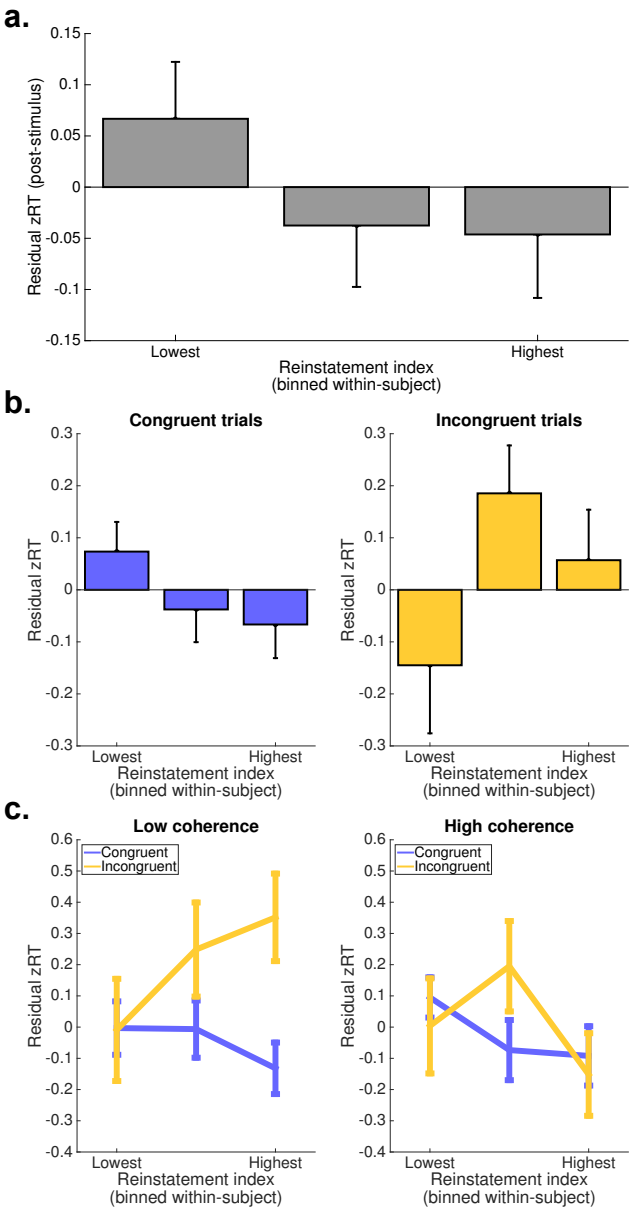

Figure 6: **Accumulated memory evidence is incorporated into perceptual evidence accumulation.** **(a)** Across all trials, a higher reinstatement index predicts faster responding after stimulus onset. After regressing out several factors that each predict RT – cue level, coherence, ISI, perceptual evidence – we observed a reliable correlation between reinstatement index and response time. At a trial-by-trial level, participants' responses were faster the more they anticipated the content of the upcoming flickering stream ($R = -0.0337$, bootstrap $P = 0.039$). **(b)** Reinstatement index speeds responses to cue-congruent, but not cue-incongruent, perceptual information. (incongruent: $R = 0.0096$, $P = 0.404$; congruent: $R = -0.0527$, $P = 0.029$; Cohen's $d = -1.2037$). **(c)** If accumulated memory evidence sets the starting point for perceptual evidence accumulation, then it should have the effect of slowing responses to unreliable perceptual evidence. Consistent with this model, we observed that, on low-coherence trials, reinstatement index slows responses to cue-incongruent stimuli. (low coherence, cue-incongruent: $R = 0.127$, bootstrap $P = 0.087$; low coherence, cue-congruent: $R = -0.0384$, bootstrap $P = 0.161$; Cohen's $d = -1.586$).

Discussion

Humans [6, 23], animals [9], and even intelligent machines [24] must rely on expectations, derived from experience, in order to act quickly and accurately [18]. While important empirical and theoretical work has described ways in which expectations influence dynamic, deliberative decisions [6, 7], these investigations have set aside the question of how the expectations themselves are set.

The evidence accumulation models used to study perceptual decisions also have roots in the study of recognition memory [3] – by definition an inference over past experiences. Recently, we showed that decisions for reward are informed in part by "samples" of relevant past experiences [11, 13, 14]. At each new choice, decision-makers brings to mind similar previous choices, and take the outcomes of those choices as evidence for one option or the other. We reasoned that a similar dynamic inference process could underlie expectations formed before the onset of perceptual decisions.

We tested this hypothesis in two experiments using a novel cue-guided perceptual inference task that separately varied the content and coherence of expectations derived from previous experience, and content and coherence of perceptual signals. Participants viewed a fractal cue followed, after a variable-length delay, by a "flickering" stream where two photographs were presented in rapid alternation, at a trial-specific ratio. Their task was to press a key corresponding to the photograph that appeared most often in the stream. Participants learned to use the cues to anticipate which photograph would be predominant in the stream, and also how difficult it would be to decide the dominant photograph on the basis of perceptual information alone. Accordingly, their responses reflected the influence of expectation-derived associations and online sensory evidence. They would, sometimes, act on the basis of expectations alone, before perceptual information was even available. These "early" responses were more likely when the cue more strongly predicted a given photograph, and also when it predicted a more difficult perceptual decision. These effects interacted – participants' decision to respond early was more affected by cue predictiveness when perceptual coherence was high.

Participant response times were best-fit by a two-stage evidence accumulation model. This model describes decisions as arising from a continuous inference process that samples evidence at one drift rate until a given deadline, and then samples evidence at a second drift rate. The critical prediction of this model is that evidence accumulated during the first stage should influence responses made during the second stage. To test this directly, we used fMRI to observe, on each trial, participants' neural responses to the cue, in anticipation of the flickering stream. This measure was indeed a reliable predictor of response times – the more participants anticipated the photograph predicted by the cue, the faster they were to respond after the onset of the perceptual stimulus. Taken together, our results demonstrate that the dynamics of expectation-setting combine with those of sensory inference to affect responses.

Previous theoretical and empirical work has outlined the normative conditions under which expectations should bias inference [6, 7], and the mechanisms by which expectations are incorporated into the decision itself [9]. Several possible mechanisms have been pro-

posed, and tested, across a range of tasks. A potential synthesis of these accounts is that expectations are themselves inferred, on the basis of memory. In the case that memories are consistent about what expectations should be, and also consistent with perceptual information, such an accumulation would appear as a static offset to the inference process; but, in cases where memory evidence is reliable, but perceptual information is inconsistent within the course of a trial, the same process could appear as a dynamic bias signal. Continuous accumulation of memory and perceptual evidence also predicts that these effects vary, qualitatively, along with the relative reliability, and consistency, of the two kinds of evidence. In perceptual sampling models, this kind of variability in decision parameters tends to be modeled as noise [25]. Here, we attempt to unpack that noise, to provide both an instrumental justification for, and a process-level explanation of, changes in the decision process.

These findings fit with a burgeoning literature on the influence of memory on decisions. Empirical work, by ourselves and others [4, 11, 13, 26, 27] has outlined a process by which decisions can be made on the basis of evidence accumulated from individual memories of past decisions (see Shohamy and Shadlen [12] for a proposal framing these findings in terms of evidence accumulation). Along this line, a key differentiating factor of our study relative to previous work is that expectations were based on a relatively small number of direct, but variable, experiences. Other investigations of expectation's influence on decision-making set expectations using either explicit instructions or extensive overtraining. This distinction highlights an important question left open by our investigation. Though we were motivated by our work on sampling from episodic memory, the current study does not directly address the involvement of individual episodes. An important next step will be to determine what is the exact content of the internal representation – or representations, such as semantic memories and motor responses – used to set expectations in this task.

Hanks and colleagues [9] evaluated how perceptual decisions can be aided by statistical regularities. They observed that priors had stronger influence as a function of the elapsed decision time on a given trial. On this basis they inferred that decision time was used as an online estimate of decision difficulty. While the study did not evaluate pre-decision activity as a function of expectations, they did observe coherent activity preceding stimulus onset; this activity was unrelated to decision outcome in their task, but this may be due to the limited amount of time available for expectations to be accumulated. The synthesis of our results with theirs implies an interesting path for future research. Specifically, while our results suggest that the weighing process they observe could begin before decision onset, theirs suggest that inference over experiences may continue in parallel, after stimulus onset. An ongoing mixture of expectations and sensory information should fit with their account when sensory information is largely congruent with expectations, but may qualitatively diverge when trial-varying expectations – observed before the onset of the perceptual stimulus – turn out to be incongruent with sensory information. A conclusive test of this hypothesis will likely require a method with finer temporal resolution than is available to fMRI, as well as wider spatial coverage than traditionally used in single-unit recording.

A tantalizing possibility is that the notion of cooperative evidence accumulation – whether in serial or in parallel – applies more broadly throughout neural computation. Though

various kinds of decisions have been modeled as arising from the competition of one or more "racing" accumulators [16, 28], the idea that multiple types of information might be sampled in a cooperative fashion, towards a single decision resolution, has been less widely investigated. Most interesting is the possibility that these two approaches – competitive and cooperative accumulation – need not be at odds, or entirely distinct. Race models are supported by the observation that response time distributions correspond to the accrued evidence for one alternative or the other, rather than the net between. A unifying explanation could be that accumulation is competitive at the level of each sensory modality or internal representation, but integrative across such inputs. For instance, ongoing samples from past experience could amplify consistent sensory evidence samples, or weigh against inconsistent ones.

A related question is how exactly it is that information is transmitted downstream from memory. One possibility is that memories provide a feedback signal that shapes processing in earlier visual regions [29]. Another, not incompatible, possibility is that accumulated memory evidence persists as a form of visual working memory. In some decisions, subjects may choose to forego further sampling, even if they have accumulated only partially to bound [10]. But the accumulated evidence may still carry forward to the later inference process. In a separate study, we examined how reinstated episodic memories persist across a delay to affect evidence accumulation in support of a simple recognition task [30]. This sort of mechanism could explain how accumulated memory information persists across delays.

This finding may have important implications for the study of decisions more broadly. Economic decisions, for instance, require integrating information about multiple attributes of the choice options. Individuals may differ in how they combine these attributes. The heuristics necessary to do so are proposed to underlie some of the observed "irrationalities" of behavioral economics, and measurements of the variation in the attention paid to different options has been shown to improve predictions of choices [31]. Here, we show how sampled memories can combine with sampled perceptual features, improving the prediction of choices over those made on the basis of either type of information alone.

More broadly, in the real world, expectations are nearly omnipresent, it is possible that previous investigations have obscured an important source of trial-by-trial variation. Decisions may often be biased by samples from internal information – memories, but also emotions, values, and rules – that give rise to expectations established in the moment, rather than fixed across time. In other words, rather than take expectations as given, our brains may treat the past as just as uncertain as the present.

Acknowledgements

The authors wish to thank Abigail Hoskin, Amitai Shenhav, Judith Fan, Phillip Holmes, Michael Waksom and Roozbeh Kiani for helpful conversations, Ghootae Kim for providing ranked face and scene stimuli, Nicholas Hindy for providing fractal stimuli, and Charlotte Townsend for extensive assistance with data collection. This publication was made possible through the support of a grant from the John Templeton Foundation (Grant ID #57876;

K.A.N. and J.D.C.). The opinions expressed in this publication are those of the authors and do not necessarily reflect the views of the John Templeton Foundation.

Contributions

A.M.B. and M.A. conceived experiment; A.M.B., M.A., and S.F.F. designed experiment and analyses, with input from N.B.T., K.A.N. and J.D.C.. A.M.B. and M.A. wrote the experiment code; A.M.B. and M.A. ran the experiment; A.M.B. and S.F.F. contributed analytic tools; A.M.B. and S.F.F. performed analyses; A.M.B. wrote the paper, with input from M.A., K.A.N., and J.D.C.. All authors approved the final manuscript.

Methods

Participants

33 participants (15 male, 30 right-handed; ages 18-50, mean 21.9) each performed two repetitions of the task in Experiment 1. Ten blocks were excluded for failing to meet one or more criteria: if the participant failed to respond on 10% of learn or test-phase trials (nine blocks); if the combined number of skipped trials and post-stimulus error trials during the test phase were greater than 30% (four blocks); if the difference between calibrated accuracies for any pair of stimuli was less than 5% (one block). Three participants failed to meet criteria for all blocks they performed; they were excluded entirely from analysis. In all, 30 participants and 56 blocks were included in the final analysis.

36 participants (10 male, 29 right-handed; ages 18-33, mean 23.19) each performed one (5) or two (31) repetitions of the task in Experiment 2. (Five blocks were excluded due to scanner malfunction (1), participant discomfort (1), or programming error (3).) 15 blocks were excluded for failing to meet one or more criteria: nine for failing to respond on enough learn or test-phase trials; one for failing to respond correctly or at all on enough test-phase trials; nine for failing the calibration accuracy threshold. Five participants failed to meet criteria for all blocks they performed; they were excluded entirely from analysis. In all, 31 participants and 52 blocks were included in the final analysis.

In Experiment 1, participants were compensated with course credit. In Experiment 2, participants were paid a flat fee of $50. All participants reported themselves as free of neurological or psychiatric disease, and fully consented to participate. The study protocol was approved by the Institutional Review Board for Human Subjects at Princeton University.

Task

The experiment was controlled by a script written in Matlab (Mathworks, Natick, MA, USA), using the Psychophysics Toolbox [32]. Both Experiment 1 and Experiment 2 consisted of the following four phases, repeated for two blocks for each participant, with different stimuli

and task conditions as detailed below. Experiment 2 was performed in an fMRI scanner, and consisted of an additional, fifth phase, a Localizer task described below.

In *Phase 1*, the *Response training* phase, particpants learned to map response keys to stimuli. Four response keys – numbers one through four on a standard US keyboard – were each associated with one of four stimuli – black and white photographs, two faces and two natural scenes.

Stimulus photographs were chosen from a set of four possible scenes and four possible faces. Each category was subdivided into two sets of two paired photographs. Each photograph was black and white, normalized for contrast and brightness, and chosen to be highly confusible with the paired face or scene.

Participants were first shown each photograph, centered on a black background, in order of the associated response keys, and asked to press the current key in the sequence. In all experiments. keys one and two corresponded to the faces, and keys three and four corresponded to scenes. Then, the photographs were shuffled, and presented one at a time for two seconds each. Participants were instructed to press the corresponding key. If they pressed the correct key, a green box appeared around the photograph. If they pressed the incorrect key, the photograph remained on the screen. Each photograph was displayed ten times. If participants pressed the incorrect key on the first try more than twice for any photograph, they were made to repeat the response training phase in its entirety.

Phase 2, the *Calibration* phase, measured the ability of participants to discriminate between each pair of photographs when they were presented in a noisy, "flickering" stream (Figure 1). On each trial, participants were shown a rapid stream of pictures, displayed for 1/60th of a second apiece. They were instructed to press the key corresponding to the *target* – the photograph shown most often. Each frame consisted of either the target photograph, the paired same-category photograph, or a perceptual mask consisting of a phase-scrambled version of the previously shown photograph. Perceptual masks were shown for between one and three frames, with mask display length chosen from a truncated, discretized exponential distribution of mean 2. Calibration trials lasted three seconds, regardless of response. When participants pressed a key, the stream stopped, and the target was shown for the remainder of the trial length. If the participant pressed the correct key, a green box appeared around the photograph. If the participant pressed the incorrect key, a red box appeared around the photograph. A one second inter-trial-interval (ITI) followed each trial. On each trial, the proportion of frames that contained the target photograph – the *coherence* – was updated according to a Quest algorithm [33], with the goal of calibrating participants responses to either 65% (low) or 85% (high) accuracy. Each block measured the coherence necessary to elicit either high or low accuracy for each photograph. In Experiment 1, the first 24 participants performed 60 calibration trials per photograph, while the last 9 participants performed 40 calibration trials per photograph. In Experiment 2, participants performed 30 calibration trials per photograph. Although Experiment 2 participants remained in the fMRI scanner for this phase, no scanner data was collected. This is the only phase for which scanner data was not collected.

In Experiment 1, for stimuli calibrated to low accuracy (65%), the average coherence

(proportion of non-mask frames that contained the target photograph), across participants, blocks, and stimuli, was 60.98% (SEM 1.06%); whereas for the high-accuracy (85%) condition, the target photograph was shown on 75.88% (SEM 1.08%) of frames. In Experiment 2, these figures were 62.17% (SEM 1.03%) coherence in the low-accuracy condition, 77.66% (SEM 1.15%) coherence in the high-accuracy condition.

Phase 3, the *Cue learning* phase, provided participants with a set of experiences that linked each of four fractal cues to the photographs (Figure 1). On each trial, participants were shown one of four fractal cues, displayed on the screen for 750ms. In Experiment 1, the cue was followed by a variable inter-stimulus-interval (ISI). For 24 participants, this ISI was either 500ms, 1000ms, or 4000 ms, selected pseudorandomly at each trial according to a uniform distribution. For the remaining 9 participants in Experiment 1, and all participants in Experiment 2, this ISI was a fixed length of one second. After the ISI, participants were shown either of two photographs linked to the cue, both from the same category (face or scene). The photographs that followed the cue were selected according to one of four binomial distributions – 50/50, 60/40, 70/30, or 80/20. The two cues in each category (face or scene) predicted their consequents using symmetric distributions – if one cue predicted Face A with 80% probability, the other cue predicted Face B with 80% probability. Participants were instructed to press the button corresponding to the displayed photograph. If the response was accurate, the photograph was surrounded by a green box. If the response was inaccurate, the photograph was surrounded by a red box. Regardless of response time or accuracy, the picture remained on the screen for two seconds. In Experiment 1, the trial was followed by an ITI of two seconds. In Experiment 2, the trial was followed by an ITI of between 500ms and 8000ms, chosen from a truncated exponential distribution, discretized in units of 500ms, with mean 2000ms. This phase consisted of 100 trials, 25 for each cue, ordered pseudorandomly.

Phase 4, the *Cued inference task*, was the primary test of our hypotheses. On each trial during this phase, participants first viewed a fractal cue that predicted the likelihood of the target photograph during the following flickering stream. Cues were presented for 750ms, and followed by an ISI of variable length, selected at each trial from a uniform distribution. For the first 24 subjects of Experiment 1, this ISI was either 500ms, 1000ms, or 4000ms. For the remaining 9 subjects of Experiment 1, this ISI was either six, eight, or ten seconds. In Experiment 2, this ISI was either four, six, or eight seconds. In both experiments, ISI durations were chosen from a uniform distribution over the possible values. The flickering stream used one of the two mixture proportions calibrated during Phase 2; mixture proportions were fixed for each category – e.g. faces might be set to low coherence, and scenes to high coherence. Thus, the fractal cue predicted both the likely identity of the target photograph, and also the coherence of the subsequent stream. The stream remained on the screen for three seconds. When a key was pressed, the target photograph appeared, and remained on the screen until the three seconds were finished. If the keypress was correct, the photograph was surrounded by a green box. If the keypress was incorrect, the photograph was surrounded by a red box. Participants were instructed to press the key corresponding to the identity of the target photograph. Critically, however, participants were allowed to

respond early – during the ISI, before the flickering stream began. Participants were not given any explicit or implicit inducement to respond early or accurately – they were informed that, regardless of the speed or correctness of their response, all trials were of fixed length, modulo the ISI. This phase continued for 80 trials, 20 trials of each cue, ordered pseudorandomly.

Phases one through four were repeated as two blocks, each with different fractal cues and picture stimuli. Cue were selected pseudorandomly for each block, and the mapping from coherence level to category was counterbalanced between blocks.

After the two blocks, Experiment 2 participants completed a final phase, *Phase 5*, the *Localizer* task. We used the data collected in this phase to localize regions of cortex preferentially active during processing of face and scene images. Participants performed a 1-back image repeat detection task. Images were presented in mini-blocks of 10 trials each. Eight of the pictures in each block were trial-unique, and two were repeats of the picture on the immediately preceding trial. Repeats were inserted pseudorandomly according to a uniform distribution. Stimuli in each mini-block were chosen from a large stimulus set of pictures not used in the main experiment. The pictures belonged to one of four categories – faces, objects, scenes or phase-scrambled scenes. Pictures were each presented for 500ms, and separated by a 1.3s ISI. A total of 12 mini-blocks were presented (3 per category), with each mini-block separated by a 12 second inter-block interval.

Imaging methods

Experiment 2 was collected while participants were laying in the fMRI scanner. Data were acquired using a 3T Siemens Prisma scanner with a 64-channel volume head coil. We collected three functional runs with a T2*-weighted gradient-echo multi-band echo-planar sequence (44 slices oriented parallel to the long axis of the hippocampus, 2.5mm isotropic resolution, echo time 26 ms; TR 1000 ms; flip angle 50 deg; field of view 192 mm). To allow for T1 equilibration, we discarded the first six volumes of each functional run (6s). We also collected a high-resolution 3D T1-weighted MPRAGE sequence (1mm isotropic resolution) for registration across participants to standard space. Functional image preprocessing was performed using FSL (FMRIB Software Library version 5.0.8; [34, 35]). Anatomical images were coregistered to the standard MNI152 template image, then individual participant functional images were coregistered to the realigned anatomical images. The transformation matrices generated during this coregistration process were used to transform Region of Interest (ROI) images (described below, *ROI definition*). Functional images were motion corrected and spatially smoothed using a 5mm full-width half-maximum Gaussian kernel prior to analysis. Data were scaled to their global mean intensity and high-pass filtered with a cutoff period of 128s.

Behavioral analysis

Response time analyses

Bimodality. We tested whether response time distributions within each ISI condition were bimodal, using Hartington's Dip Test [17]. This test measures the relative spread between modes to the mean of the distribution – larger values indicate a higher likelihood of true bimodality in the tested data. P-values are estimated via bootstrap against distributions with the same summary statistics as the tested data, provided by the MATLAB function HartigansDipTest [36].

Permutation tests for across-condition correlations. Each participant performed a different subset of the task conditions (cue level, perceptual coherence). To provide a robust measure of the relationship between response times and conditions, we therefore performed a bootstrap analysis, across participants and conditions [37]. On each iteration, we sampled, with replacement, the number of participants in the study group (33 in Experiment 1, 33 in Experiment 2). We then computed, on this selected group, the correlation of interest. By repeating the process 10,000 times, we obtained a distribution of correlation values across shuffled permutations of the study group. The reported p-value is thus the fraction of correlation values with a different sign from the base effect size (the correlation across the entire original group). We also leveraged these shuffled permutations to measure the difference between correlations across conditions (coherence levels, early versus late responses). To do this, we performed the paired bootstrap analyses using the same set of 10,000 permutations – each permutation of participants was matched between the two correlations. We then measured the effect size using Cohen's d [38]; by convention effect sizes measured in this way greater than 0.80 are "Large", and likely reliable.

Model comparison

Multi-stage DDM. Our primary model of interest is an extension of the drift-diffusion model [3] to allow for a time-varying drift rate [15]. The model specifies drift rate as a time-varying, piecewise constant function – each shift in drift rate defines a separate stage of the accumulation process. Critically, the endpoint of one stage leads to the starting point of the next. Our instantiation used two stages. The free parameters were the drift rates, d_1 and d_2, threshold a, non-decision time T_0, and starting point x_0. We refer to this model as *MSDDM*.

Our comparison models were matched to this MS-DDM in parameters, with selective disabling of each key feature – the time-varying drift rate, and the connection between stages. The first comparison model of interest was a single DDM, with continuous accumulation until the time of response, but no change in drift rate across the entire period between cue onset and response. We refer to this model as *1DDM*, with free parameters d_1, a, T_0, and x_0. The second comparison model of interest was two DDMs, each fit to pre-stimulus and post-stimulus responses separately and thus mirroring the change in drift rate found in MS-DDM, but with the second starting point its own free parameter. We refer to this model as *2DDM*, with free parameters d_1, d_2, a, T_0, and starting points $x_{0,1}$ and $x_{0,2}$. Each model was fit to participant responses aggregated according to cue and coherence

condition, and the summed residuals across conditions were used to calculate likelihood. The Bayesian Information Criterion (BIC; [39]) was used to compare likelihoods across models, while penalizing more complex models for their additional parameters.

Imaging analysis

To identify neural markers of stimulus reinstatement, we first defined patterns of activity in ventral visual stream regions that indicated participants were processing "face" or "scene" photographs. We then analyzed the degree to which these patterns were present during the post-cue, pre-stimulus ISIs in Phase 4. Because no pictures were present on-screen during this period of interest, we reasoned that greater evidence of stimulus reinstatement would indicate that participants were recalling the cued photograph. We therefore predicted that this reinstatement evidence would be reflected in response accuracies, response times, and DDM model parameters.

ROI definition. We identified a region of interest consisting of voxels that (across the group) showed preferential activation to face or scene photographs, using the following procedure.

First, for each participant, we performed a GLM analysis of BOLD signal during the localizer task. We identified voxels that responded more to scenes or faces, relative to other categories (univariate contrasts: faces > scenes | scrambled_scenes | objects; scenes > faces | scrambled_scenes | objects). For each participant, we selected clusters in the posterior parahippocampal region (matching the reported Parahippocampal Place Area (PPA); [21]) and posterior fusiform gyrus (matching the reported Fusiform Face Area (FFA); [20]) that were significant at $p < 0.005$, uncorrected. Next, each per-participant voxel mask was binarized; all above-threshold voxels were set to 1. To regularize the ROIs and ensure they were consistent across subjects, the resulting individual mask was then warped to match the group average anatomical; these group-space masks were added together and the summed image thresholded to include all voxels present in more than 90% of participants. This final group ROI was then warped back to the individual participant space, and the result used as the final mask for pattern analysis.

Stimulus-specific pattern analysis. We computed the pattern of activity for each target photograph, across the corresponding category-preferring ROI. For each photograph in each block, we took the average pattern of activity over the last five presentations of the photograph during Phase 1. (The first five presentations were excluded to allow repetition suppression and learning effects to stabilize.)

We next used these four three-dimensional patterns as a template for analyzing activity during the post-cue, pre-stimulus ISI in Phase 4. For each trial, we computed, within the ROI corresponding to the cued category, the pattern of activity between the time of cue onset and the time of response or one TR before the onset of the flickering stream, whichever came first. We then correlated this three-dimensional activity pattern with each of the the same-category patterns defined as above. We refer to this correlation value as the *reinstatement index*.

These correlation values, one for each Phase 4 trial, were then fisher-transformed and used as predictor variables in our analyses of interest.

References

[1] Antonio Rangel, Colin Camerer, and P Read Montague. A framework for studying the neurobiology of value-based decision making. *Nature Reviews Neuroscience*, 9(7):545–56, jul 2008. ISSN 1471-0048. doi: 10.1038/nrn2357. URL http://www.ncbi.nlm.nih.gov/pubmed/18545266.

[2] Joshua I Gold and Michael N Shadlen. The neural basis of decision making. *Annual Review of Neuroscience*, 30:535–74, jan 2007. ISSN 0147-006X. doi: 10.1146/annurev.neuro.29.051605.113038. URL http://www.ncbi.nlm.nih.gov/pubmed/17600525.

[3] Roger Ratcliff. A Theory of Memory Retrieval. *Psychological Review*, 85(2):59–108, 1978.

[4] Alan M Gordon, Jesse Rissman, Roozbeh Kiani, and Anthony D Wagner. Cortical Reinstatement Mediates the Relationship Between Content-Specific Encoding Activity and Subsequent Recollection Decisions. *Cerebral Cortex*, 24(12): 3350–3364, aug 2013. ISSN 1460-2199. doi: 10.1093/cercor/bht194. URL http://www.ncbi.nlm.nih.gov/pubmed/23921785.

[5] Don van Ravenzwaaij, Martijn J Mulder, Francis Tuerlinckx, and Eric-Jan Wagenmakers. Do the dynamics of prior information depend on task context? An analysis of optimal performance and an empirical test. *Frontiers in psychology*, 3(May):132, jan 2012. ISSN 1664-1078. doi: 10.3389/fpsyg.2012.00132.

[6] Jan Drugowitsch, Rubén Moreno-Bote, Anne K Churchland, Michael N Shadlen, and Alexandre Pouget. The cost of accumulating evidence in perceptual decision making. *Journal of Neuroscience*, 32(11):3612–28, mar 2012. ISSN 1529-2401. doi: 10.1523/JNEUROSCI.4010-11.2012. URL http://www.ncbi.nlm.nih.gov/pubmed/22423085.

[7] Rani Moran. Optimal decision making in heterogeneous and biased environments. *Psychonomic Bulletin & Review*, pages 38–53, 2015. doi: 10.3758/s13423-014-0669-3.

[8] Don Van Ravenzwaaij, Martijn J Mulder, Francis Tuerlinckx, and Eric Jan Wagenmakers. Paradoxes of Optimal Decision Making : A Response to Moran (2015). *Psychonomic Bulletin & Review*, 22:307–308, 2015.

[9] Timothy D. Hanks, Mark E. Mazurek, Roozbeh Kiani, Elizabeth Hopp, N Michael, and M. N. Shadlen. Elapsed Decision Time Affects the Weighting of Prior Probability in a Perceptual Decision Task. *Journal of Neuroscience*, 31(17):6339–6352, apr 2011. ISSN 0270-6474. doi: 10.1523/JNEUROSCI.5613-10.2011. URL http://www.jneurosci.org/cgi/doi/10.1523/JNEUROSCI.5613-10.2011.

[10] Rajesh P. N. Rao. Decision Making Under Uncertainty: A Neural Model Based on Partially Observable Markov Decision Processes. *Frontiers in Computational Neuroscience*, 4:1–18, 2010. ISSN 1662-5188. doi: 10.3389/fncom.2010.00146. URL http://www.frontiersin.org/Computational_Neuroscience/10.3389/fncom.2010.00146/abstr

[11] Aaron M. Bornstein and Nathaniel D. Daw. Cortical and Hippocampal Correlates of Deliberation During Model-Based Decisions for Rewards in Humans. *PLoS Computational Biology*, 9(12):e1003387, dec 2013. ISSN 1553-7358. doi: 10.1371/journal.pcbi.1003387. URL http://dx.plos.org/10.1371/journal.pcbi.1003387.

[12] Michael N Shadlen and Daphna Shohamy. Decision Making and Sequential Sampling from Memory. *Neuron*, 90(5):927–939, 2016. ISSN 0896-6273. doi: 10.1016/j.neuron.2016.04.036. URL http://dx.doi.org/10.1016/j.neuron.2016.04.036.

[13] Aaron M Bornstein, Mel W Khaw, Daphna Shohamy, and Nathaniel D. Daw. What's past is present: Reminders of past choices bias decisions for reward in humans. *Nature Communications*, 2017. doi: 10.1101/033910.

[14] Aaron M Bornstein and Kenneth A Norman. Putting value in context: A role for context memory in decisions for reward. *Nature Neuroscience*, 2017. doi: 10.1101/033662.

[15] Vaibhav Srivastava, Samuel F. Feng, Jonathan D. Cohen, Naomi Ehrich Leonard, and Amitai Shenhav. A martingale analysis of first passage times of time-dependent Wiener diffusion models. *Journal of Mathematical Psychology*, 2016. ISSN 00222496. doi: 10.1016/j.jmp.2016.10.001. URL http://dx.doi.org/10.1016/j.jmp.2016.10.001.

[16] Scott D. Brown and Andrew Heathcote. The simplest complete model of choice response time: Linear ballistic accumulation. *Cognitive Psychology*, 57(3):153–178, 2008. ISSN 00100285. doi: 10.1016/j.cogpsych.2007.12.002.

[17] J. a. Hartigan and P. M. Hartigan. The Dip Test of Unimodality. *The Annals of Statistics*, 13(1):70–84, 1985. ISSN 0090-5364. doi: 10.1214/aos/1176346577.

[18] Rafal Bogacz, Eric Brown, Jeff Moehlis, Philip Holmes, and Jonathan D Cohen. The physics of optimal decision making: a formal analysis of models of performance in two-alternative forced-choice tasks. *Psychological Review*, 113(4): 700–65, oct 2006. ISSN 0033-295X. doi: 10.1037/0033-295X.113.4.700. URL http://www.ncbi.nlm.nih.gov/pubmed/17014301.

[19] R E Kass and A E Raftery. Bayes Factors. *Journal of the American Statistical Association*, 90(430):773–795, 1995.

[20] Nancy Kanwisher, Josh Mcdermott, and Marvin M Chun. The Fusiform Face Area: A Module in Human Extrastriate Cortex Specialized for Face Perception. *Journal of Neuroscience*, 17(11):4302–4311, 1997.

[21] R Epstein and N Kanwisher. A cortical representation of the local visual environment. *Nature*, 392(6676):598–601, apr 1998. ISSN 0028-0836. doi: 10.1038/33402. URL http://www.ncbi.nlm.nih.gov/pubmed/9560155.

[22] Zeb Kurth-Nelson, Gareth Barnes, Dino Sejdinovic, Ray Dolan, and Peter Dayan. Temporal structure in associative retrieval. *eLife*, 4: 1–18, 2015. ISSN 2050-084X. doi: 10.7554/eLife.04919. URL http://elifesciences.org/lookup/doi/10.7554/eLife.04919.

[23] Rafal Bogacz, Peter T Hu, Philip J Holmes, and Jonathan D Cohen. Do humans produce the speed-accuracy trade-off that maximizes reward rate? *Quarterly Journal of Experimental Psychology*, 63(5):863–91, 2010. ISSN 1747-0226. doi: 10.1080/17470210903091643.

[24] C. M. Bishop. *Pattern Recognition and Machine Learning*. Springer, London, 2006.

[25] Roger Ratcliff. Parameter variability and distributional assumptions in the diffusion model. *Psychological review*, 120(1):281–92, jan 2013. ISSN 1939-1471. doi: 10.1037/a0030775. URL http://www.ncbi.nlm.nih.gov/pubmed/23148742.

[26] Aaron M. Bornstein and Nathaniel D. Daw. Dissociating hippocampal and striatal contributions to sequential prediction learning. *European Journal of Neuroscience*, 35 (7):1011–1023, apr 2012. ISSN 0953816X. doi: 10.1111/j.1460-9568.2011.07920.x. URL http://doi.wiley.com/10.1111/j.1460-9568.2011.07920.x.

[27] Michael L Mack and Alison R Preston. NeuroImage Decisions about the past are guided by reinstatement of speci fi c memories in the hippocampus and perirhinal cortex. *NeuroImage*, 127:144–157, 2016. ISSN 1053-8119. doi: 10.1016/j.neuroimage.2015.12.015. URL http://dx.doi.org/10.1016/j.neuroimage.2015.12.015.

[28] Roger Ratcliff and Jeffrey J Starns. Modeling confidence judgments, response times, and multiple choices in decision making: recognition memory and motion discrimination. *Psychological review*, 120(3):697–719, jul 2013. ISSN 1939-1471. doi: 10.1037/a0033152. URL http://www.ncbi.nlm.nih.gov/pubmed/23915088.

[29] David J Heeger. Theory of cortical function. *Proceedings of the National Academy of Sciences*, 114(8), 2017. ISSN 0027-8424. doi: 10.1073/pnas.1619788114.

[30] AN Hoskin, Aaron M. Bornstein, Kenneth A. Norman, and Jonathan D. Cohen. Resting reinstatements from episodic memory alter the content of working memory. *bioRxiv*, 2017.

[31] Ian Krajbich, Carrie Armel, and Antonio Rangel. Visual fixations and the computation and comparison of value in simple choice. *Nature Neuroscience*, 13(10):1292–8, oct 2010. ISSN 1546-1726. doi: 10.1038/nn.2635. URL http://www.ncbi.nlm.nih.gov/pubmed/20835253.

[32] D H Brainard. The Psychophysics Toolbox. *Spatial Vision*, 10(4):433–6, jan 1997. ISSN 0169-1015. URL `http://www.ncbi.nlm.nih.gov/pubmed/9176952`.

[33] A. B. Watson and Dennis G. Pelli. QUEST: A Bayesian adaptive psychometric method. *Perception & Psychophysics*, 33(2):113–120, 1983.

[34] Stephen M. Smith, Mark Jenkinson, Mark W. Woolrich, Christian F. Beckmann, Timothy E J Behrens, Heidi Johansen-Berg, Peter R. Bannister, Marilena De Luca, Ivana Drobnjak, David E. Flitney, Rami K. Niazy, James Saunders, John Vickers, Yongyue Zhang, Nicola De Stefano, J. Michael Brady, and Paul M. Matthews. Advances in functional and structural MR image analysis and implementation as FSL. *NeuroImage*, 23 (SUPPL. 1):208–219, 2004. ISSN 10538119. doi: 10.1016/j.neuroimage.2004.07.051.

[35] Mark Jenkinson, Christian F. Beckmann, Timothy E J Behrens, Mark W. Woolrich, and Stephen M. Smith. FSL. *NeuroImage*, 62(2):782–790, 2012. ISSN 10538119. doi: 10.1016/j.neuroimage.2011.09.015.

[36] Nicholas Price and F. Mechler. HartigansDipTest, 2002. URL `http://www.nicprice.net/diptest/`.

[37] Ghootae Kim, Jarrod A Lewis-peacock, Kenneth A Norman, and Nicholas B Turk-browne. Pruning of memories by context-based prediction error. *Proceedings of the National Academy of Sciences*, 111(24), 2014. doi: 10.1073/pnas.1319438111.

[38] Jacob Cohen. *Statistical power analysis for the behavioural sciences*. NJ: Lawrence Earlbaum Associates, Hillside, NJ, 1988.

[39] Gideon Schwarz. Estimating the Dimension of a Model. *Annals of Statistics*, 6(2): 461–464, 1978.